Available online at www.sciencedirect.com
SCIENCE DIRECT
International Journal of Pharmaceutics 313 (2006) 87–98
INTERNATIONAL JOURNAL OF PHARMACEUTICS
www.elsevier.com/locate/ijpharm

Dehydration of trehalose dihydrate at low relative humidity and ambient temperature

Matthew D. Jones [a], Jennifer C. Hooton [a,1], Michelle L. Dawson [b], Alan R. Ferrie [b], Robert Price [a,*]

[a] *Pharmaceutical Surface Science Research Group, Department of Pharmacy and Pharmacology, University of Bath, Bath BA2 7AY, UK*
[b] *Inhalation Product Development, GlaxoSmithKline Research and Development, Park Road, Ware, Herts SG12 0DP, UK*

Received 31 August 2005; received in revised form 16 December 2005; accepted 18 January 2006
Available online 28 February 2006

Abstract

The physico-chemical behaviour of trehalose dihydrate during storage at low relative humidity and ambient temperature was investigated, using a combination of techniques commonly employed in pharmaceutical research. Weight loss, water content determinations, differential scanning calorimetry and X-ray powder diffraction showed that at low relative humidity (0.1% RH) and ambient temperature (25 °C) trehalose dihydrate dehydrates forming the α-polymorph. Physical examination of trehalose particles by scanning electron microscopy and of the dominant growth faces of trehalose crystals by environmentally controlled atomic force microscopy revealed significant changes in surface morphology upon partial dehydration, in particular the formation of cracks. These changes were not fully reversible upon complete rehydration at 50% RH. These findings should be considered when trehalose dihydrate is used as a pharmaceutical excipient in situations where surface properties are key to behaviour, for example as a carrier in a dry powder inhalation formulations, as morphological changes under common processing or storage conditions may lead to variations in formulation performance.

Keywords: Atomic force microscopy; Crystals; Dry powder inhalers (DPIs); Polymorphism; Surface morphology; Transition

1. Introduction

α,α-Trehalose, the disaccharide of α-D-glucose, is a naturally occurring sugar thought to confer anhydrobiotic properties (the ability to survive desiccation for long periods of time and rapidly resume metabolism upon rehydration) on various organisms in which it is found (Sussich et al., 2001). The observation of this property has led to its investigation as a stabilising excipient for the formulation of labile biological molecules and liposomes (McGarvey et al., 2003). Trehalose has also been studied as a potential carrier for dry powder inhalation formulations (Cline and Dalby, 2002; Hooton et al., in press; Naini et al., 1998).

The polymorphism of α,α-trehalose has been the subject of intense research in recent times. In addition to the dihydrate, the crystal structure of which has been known since the early 1970s (Brown et al., 1972; Taga et al., 1972), up to four anhydrous polymorphs have been identified. Of these, the β-form is the best characterised, with a known crystal structure (Jeffrey and Nanni, 1985). It can be formed from trehalose dihydrate by heating at 130 °C for 4 h (Reisener et al., 1962) or heating in a calorimeter under highly humid conditions, when it forms at 90 °C (Furuki et al., 2005). It can also be formed by a cold crystallisation of the glassy amorphous state or by a solid–solid transition from the γ anhydrous form within a calorimeter (Sussich et al., 2002). The α anhydrous form (also referred to by some authors as the K-form or form II) is produced from the dihydrate by a slow thermal dehydration or supercritical CO_2 fluid extraction of the water of crystallisation (Nagase et al., 2003; Willart et al., 2003). It has been proposed that thermal treatment of trehalose dihydrate produces the α-form when it induces the removal of water at a rate below a certain threshold level; above this, the amorphous phase is produced (Willart et al., 2003). The γ anhydrous form is only produced in a calorimeter under certain conditions, when at about 115 °C, a cold crystallisation follows partial dehydration

* Corresponding author. Tel.: +44 1225 383644; fax: +44 1225 386114.
E-mail address: R.Price@bath.ac.uk (R. Price).
[1] Present address: AstraZeneca PAR&D, Charter Way, Macclesfield, Cheshire SK10 2NA, UK.

0378-5173/$ – see front matter © 2006 Elsevier B.V. All rights reserved.
doi:10.1016/j.ijpharm.2006.01.026

of the dihydrate (Sussich et al., 1999). It is thought that this polymorph is made up of crystals with a dihydrate core surrounded by a layer of the β-form. Finally, a recent publication reports the discovery of a new anhydrous polymorph of trehalose, the ε-form (Furuki et al., 2005). This was formed by thermal dehydration in a calorimeter in an atmosphere with a partial water vapour pressure of 3–5 kPa.

This paper reports the results of investigations carried out following the observation of the unusual behaviour of trehalose dihydrate during dynamic vapour sorption (DVS) experiments. The first stage of a typical DVS protocol is the drying of the sample at 0% RH and 25 °C. Under these conditions, sugars typically lose <1% of their initial mass before reaching equilibrium, whereas trehalose dihydrate was found to lose >9% of its initial mass, prompting further enquiries to ascertain what was causing this unusual phenomenon.

2. Materials and methods

2.1. Materials

α,α-Trehalose dihydrate was obtained from British Sugar (Peterborough, UK). As supplied, the material had a polydisperse particle size distribution and since particle size is known to affect the dehydration of trehalose dihydrate (Taylor et al., 1998; Taylor and York, 1998a,b), the powder was sieved and the <63 μm fraction used for subsequent experiments. Cyclohexane and ethanol (analytical grade) were supplied by Fisher Scientific UK (Loughborough, UK) and water was prepared by reverse osmosis (MilliQ, Millipore, Molsheim, France). Lecithin was supplied by Acros Organics (Geel, Belgium). Karl Fischer anolyte solution was supplied by Sigma–Aldrich Co. Ltd. (Gillingham, UK) and Karl Fischer catholyte solution was supplied by Fisher Scientific UK (Loughborough, UK).

2.2. Methods

2.2.1. Exposure of trehalose dihydrate to dry conditions

For each exposure, approximately 150 mg of trehalose dihydrate was loaded into the sample pan of a DVS-1 instrument (Surface Measurement Systems Ltd., London, UK). The instrument was programmed to expose the sample to 0% RH at 25 °C and to continuously record sample mass, temperature and relative humidity. This continued until the rate of change of the mass of the sample reached 0%, at which point the sample was removed from the instrument and immediately subjected to further characterisation.

2.2.2. Differential scanning calorimetry

Differential scanning calorimetry (DSC) was performed with a DSC 2910 instrument (TA Instruments, Surrey, UK), calibrated with indium and tin standards. Approximately 6 mg of sample was loaded into an open aluminium pan and scanned from 30 to 230 °C at 5 °C min^{-1}. The calorimeter head was flushed with nitrogen gas at 25 ml·min^{-1} during all measurements.

2.2.3. X-ray powder diffraction

X-ray powder diffraction (XRPD) spectra were obtained using a Phillips analytical X-ray powder diffractometer (Cambridge, UK) with a CuK_α source ($\lambda = 1.5418$ Å) operated at 40 kV and 25 mA. A single sweep between diffraction angles (2θ) 5° and 30° was employed for each measurement.

2.2.4. Karl Fischer moisture titration

The total water content of trehalose before and after exposure to low humidity was determined using Karl Fischer coulometric moisture titration. Ten to twenty milligrams of each sample was accurately weighed into the titration cell of a MKC-510 Karl Fischer coulometric moisture titrator (Kyoto Electronics, Tokyo) and analysed to determine the % (w/w) water content of the sample. The total water content of three aliquots of each sample was determined in this way and the mean and standard deviation (S.D.) calculated.

2.2.5. Particle size analysis

Sample particle size was determined by laser diffraction using a Malvern Mastersizer X (Malvern Instruments Ltd., Malvern, UK) equipped with a small volume stirred cell and 100 mm lens. A small amount of the sample was suspended in a 1 mg/ml lecithin solution in cyclohexane and sonicated for 5 min prior to drop-wise addition to the sample cell. The particle size of five aliquots taken from different parts of the powder bed of each sample were measured in this way and the data combined and analysed by the instrument software to give a distribution by volume.

2.2.6. Scanning electron microscopy

Scanning electron microscopy (SEM) was used to investigate particle morphology. Samples were coated with gold using a splutter coater (model S150B, Edwards High Vacuum, Sussex, UK) and examined using a scanning electron microscope (model JEOL 6310, Japanese Electron Optics Ltd., Tokyo, Japan) at 10 keV.

2.2.7. Environmentally controlled atomic force microscopy

The effect of relative humidity on the surface topography of trehalose dihydrate crystals was investigated using environmentally controlled atomic force microscopy (EC-AFM). To ensure that any topographical changes were easily observed, the supplied trehalose dihydrate was recrystallised to produce crystals with smooth surfaces, by precipitation from a saturated aqueous solution using ethanol as an antisolvent. Crystals produced in this manner were analysed by DSC (30–300 °C) and Karl Fischer moisture titration to identify the trehalose polymorph produced.

AFM imaging was carried out in Tapping Mode® using a Multimode AFM, J-type scanner, Nanoscope IIIa controller (all from Veeco, Cambridge, UK) and a silicon tapping tip (OMCL-AC240TS, Olympus, Japan) to image 10 μm × 10 μm square areas of the crystal surface with a high resolution of 512 × 512 pixels and a scan rate of 1 Hz. The AFM head was enclosed and perfused with nitrogen of a controlled humidity, as described

elsewhere (Price et al., 2002). A sensitive humidity and temperature sensor (Rotronic AG, Bassersdorf, Switzerland) within the AFM head enabled the environmental conditions in the sample area to be monitored.

A crystal of trehalose dihydrate was mounted on an AFM stub and positioned in the instrument. A visually smooth area of its dominant face was imaged under ambient conditions (22 °C and 35% RH) before the relative humidity of the EC-AFM head was rapidly reduced to <1% RH (at 22 ± 1 °C) whilst continuously imaging the same area of the crystal surface. When no further topographical changes were observed, the humidity of the AFM head was rapidly increased to 50 ± 3% RH (at 22 ± 1 °C); imaging continued until no further changes were observed. The crystal was then removed from the AFM and rapidly transferred to the SEM for imaging. In another experiment, the crystal was removed after reaching topographical stasis at <1% RH and immediately imaged using SEM.

Using these conditions, each EC-AFM image was completed in 8.58 min by raster scanning the imaged area. As described in greater detail elsewhere (Price and Young, 2004), it is important to consider the scan direction and lag time between the top and bottom of each image. All images presented here were therefore recorded in the downward scan direction.

The roughness of each image was quantified using the root mean square of the variations in the height of the imaged surface (rugosity, R_q), as calculated by the AFM software.

2.2.8. Dynamic vapour sorption

DVS was employed to study the effect of the conditions encountered during EC-AFM on the recrystallised trehalose. Approximately 150 mg of recrystallised trehalose (approximately 30 crystals) was loaded into the sample pan of a DVS-1 instrument (Surface Measurement Systems Ltd., London, UK) and its mass continually recorded whilst subjected to a relative humidity cycle designed to mimic that used during EC-AFM. This cycle consisted of 15 min equilibration at 35% RH, followed by 3 h at 0% RH and finally 2 h at 50% RH. The temperature of the instrument was maintained at 22 °C throughout the experiment, to mimic the temperature encountered during EC-AFM. Transmission light micrographs of representative trehalose crystals before and after exposure to this DVS cycle were recorded using a 2.5× lens and CCD camera.

3. Results

3.1. Effect of low humidity on mass of trehalose dihydrate

The temperature and humidity within the DVS instrument were maintained at 25.0 ± 0.2 °C and 0.1 ± 0.1% RH throughout each exposure of trehalose dihydrate to low humidity. As Fig. 1 shows, the mass of trehalose decreased steadily after introduction into the low humidity conditions within the DVS instrument. After approximately 2000 min, equilibrium was reached at 9.43% mass loss, which is virtually equal to the loss of mass seen upon the complete dehydration of trehalose dihydrate (9.52%) (Sussich et al., 1998).

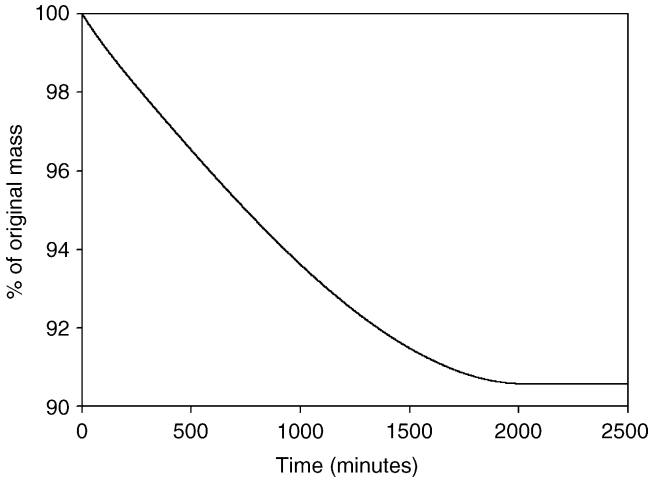

Fig. 1. Example of trehalose dihydrate mass loss as a function of time since exposure to 0.1% RH at 25 °C.

3.2. Differential scanning calorimetry

The thermograms obtained from <63 μm sieve fraction trehalose samples before and after exposure to low humidity are shown in Fig. 2. Comparison of the pre-low humidity thermogram with those in the literature obtained under the same DSC conditions (Sussich et al., 2002; Willart et al., 2002) confirmed the material's identity to be trehalose dihydrate. The large endotherm between 60 and 114 °C represents dehydration and is followed by a very weak endotherm between 120 and 135 °C representing the glass transition of resultant amorphous phase. Between 165 and 220 °C, a large exotherm is immediately followed by a sharp endotherm, corresponding to the crystallisation and then melting of β anhydrous trehalose.

The trehalose thermogram obtained after exposure to low humidity is different to that of trehalose dihydrate (described above) and similar to those in the literature obtained from α anhydrous trehalose using the same DSC conditions (Willart et al., 2002). There is a weak endotherm between 120 and

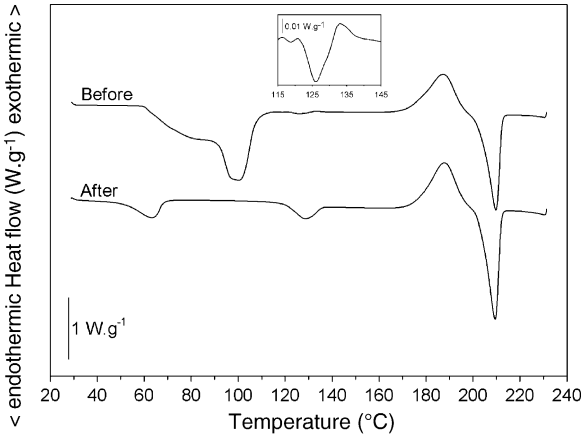

Fig. 2. DSC thermograms obtained from <63 μm sieve fraction trehalose samples before (upper thermogram) and after (lower thermogram) exposure to low humidity. The inset shows an expanded view of the 115–145 °C range of the upper thermogram.

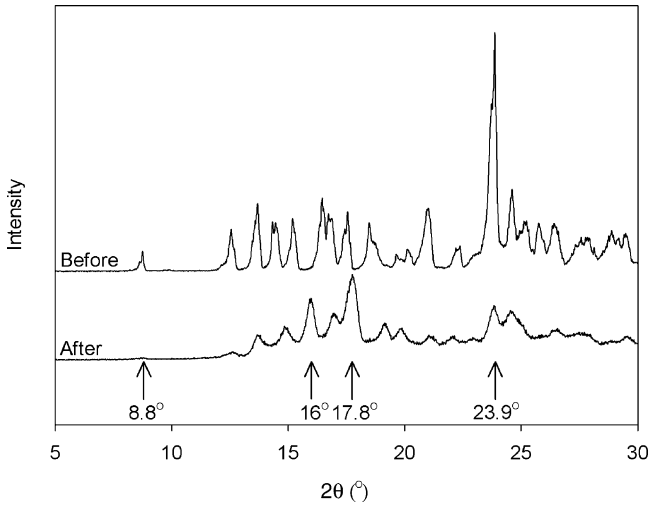

Fig. 3. XRPD spectra of <63 μm sieve fraction trehalose sample before (upper spectrum) and after (lower spectrum) exposure to low humidity. Labels show position of peaks characteristic of dihydrate or α anhydrous polymorphs of trehalose.

140 °C, which is both larger and at a slightly higher temperature than that corresponding to the glass transition of the amorphous form that was observed in the thermogram of trehalose dihydrate. This endotherm may therefore correspond to the melting of the α-form (Willart et al., 2002). Once again, there is a large exotherm and followed by a sharp endotherm between 165 and 220 °C, representing the recrystallisation and subsequent melting of the β-form. There is, however, also a weak endotherm between 50 and 70 °C, which presumably represents dehydration, although its enthalpy is only 9.99% of the dehydration enthalpy seen in the trehalose dihydrate thermogram.

3.3. X-ray powder diffraction

Fig. 3 shows the XRPD spectra obtained from <63 μm sieve fraction trehalose samples before and after exposure to low humidity. The spectrum obtained before exposure to low humidity is clearly comparable to those in the literature relating to trehalose dihydrate. In particular, it shows an intense peak at 23.9° and a small peak at 8.8°, both of which are not seen in spectra obtained from any other trehalose polymorph (Furuki et al., 2005; Nagase et al., 2002; Taylor and York, 1998a). Exposure of trehalose to low humidity conditions causes significant changes to its XRPD spectrum. The new spectra is similar to those in the literature obtained from the α anhydrous form of trehalose, containing peaks at 16.0° and 17.8° that are characteristic only this polymorph (Furuki et al., 2005; Nagase et al., 2002). There is a small upward deviation in the baseline at 8.8° and also a small peak at 23.9°, suggesting that the sample might also contain a small amount of trehalose dihydrate. Neither spectrum is comparable to published spectra of the β-form of trehalose, as they lack the peaks at 6.7°, 20.5° and 22.5° that are characteristic only of this polymorph (Furuki et al., 2005).

Table 1
Particle size descriptors of <63 μm sieve fraction trehalose samples before and after exposure to low humidity

	$D_{10\%}$ (μm)	$D_{50\%}$ (μm)	$D_{90\%}$ (μm)
Before low humidity	2.76	16.83	59.52
After low humidity	2.66	17.07	58.75

3.4. Karl Fischer moisture titration

The mean total water content of the <63 μm sieve fraction of trehalose before exposure to low humidity was 9.73% (w/w) (S.D. = 0.13% (w/w)), suggesting that the sample was trehalose dihydrate (water of crystallisation content = 9.52% (w/w) (Sussich et al., 1998)) with a small amount of water adsorbed to its surface, as the sample had been stored under ambient laboratory conditions (approximately 31% RH and 24 °C). The mean total water content of the <63 μm sieve fraction of trehalose after exposure to low humidity was 0.47% (w/w) (standard deviation 0.19% (w/w)). Assuming that there was no water adsorbed to the surface of the samples, this suggests that exposure of trehalose dihydrate to low humidity removed >95% of the water of crystallisation.

3.5. Particle size analysis

Particle size descriptors of the <63 μm sieve fraction trehalose samples before and after exposure to low humidity are shown in Table 1. The similarity of the distributions suggests that low humidity treatment did not affect trehalose particle size.

3.6. Scanning electron microscopy

Representative SEM images of the surfaces of trehalose particles in the <63 μm sieve fraction before and after exposure to low humidity are shown in Fig. 4. These show that the starting material had relatively smooth surfaces with adhered fine particles (Fig. 4(A) and (B)), whereas after exposure to low humidity an irregular system of interconnected cracks had opened in the surface of both the large particles and the adhered fines (Fig. 4(C) and (D)).

3.7. Environmentally controlled atomic force microscopy

The recrystallisation of trehalose produced crystals approximately 2 mm × 1 mm × 1 mm in size (see Fig. 5) containing 9.96% (w/w) (S.D. = 0.44% (w/w), $n = 3$) water as analysed by Karl Fischer moisture titration, suggesting the crystals to be trehalose dihydrate (9.52% (w/w) water content (Sussich et al., 1998)), as would be expected given the recrystallisation method (Brown et al., 1972). A typical single crystal DSC thermogram obtained from this material is shown in Fig. 6. This is significantly different from those obtained from trehalose powder samples (volume median diameter ≈ 17 μm, see Fig. 2), however, this is to be expected given the difference in the particle size of the two materials and the effect this is known to have on trehalose thermograms (Taylor and York, 1998a). The thermogram

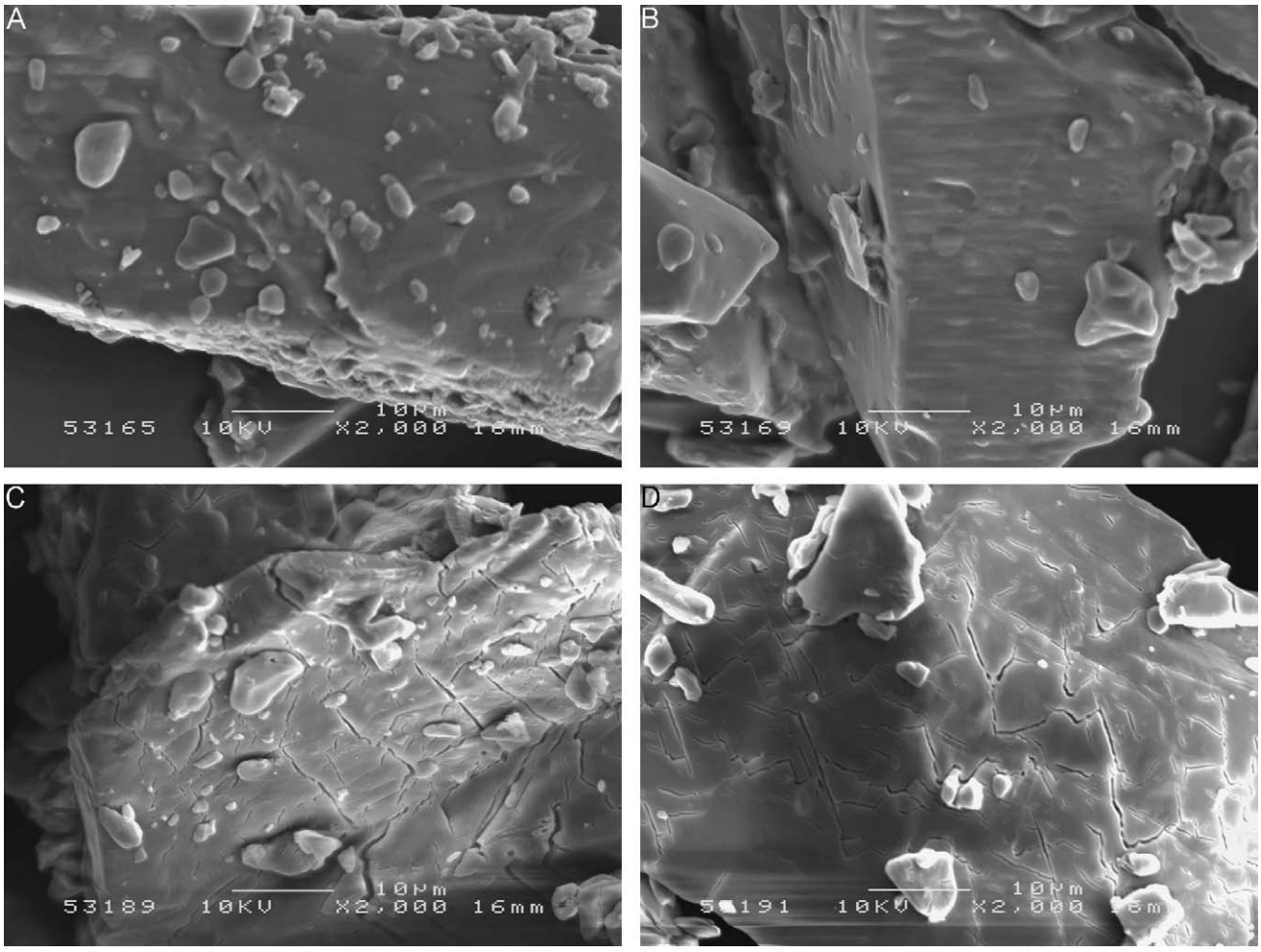

Fig. 4. Representative SEM images of the surfaces of trehalose particles before (A and B) and after (C and D) exposure to low humidity.

shows a large, sharp endotherm at 101.6 °C, which is comparable to the dehydration peak seen at this temperature in thermograms of a >425 μm sieve fraction of trehalose dihydrate (Taylor and York, 1998a), suggesting the recrystallised material is itself trehalose dihydrate. There is then a broad, irregular endotherm between 122 and 175 °C, which is not seen in the published thermograms of a >425 μm sieve fraction of trehalose dihydrate, although a similar peak does occur between 110 and 125 °C in such thermograms (Taylor and York, 1998a). The absence of peaks associated with the crystallisation and melting of β anhydrous trehalose between 165 and 220 °C should also be noted. There is however a broad endotherm between 220 and 270 °C, which may represent the melting to the β-form. If this were the case, crystallisation to the β-form might have occurred over a broad range of temperatures without producing a noticeable exothermic peak, as has previously been observed in certain situations (Sussich et al., 2002). Although no attempt is made to explain these anomalous observations, they are presumably related to the well-characterised effect that particle size has on the pathway and kinetics of the polymorphic transformations of trehalose (Taylor et al., 1998; Taylor and York, 1998a,b).

AFM Tapping Mode® images and cross-sections of the surface of the recrystallised trehalose dihydrate crystals under ambient conditions revealed a generally smooth surface (approximately 4 nm between highest and lowest points of cross-section, R_q = 1.115 nm, Fig. 7(A)), which was initially stable upon exposure to low humidity. After approximately 30 min at <1% RH, surface morphology began to show changes, initially in the form of small, irregularly shaped indentations (Fig. 7(B)). Over the next 30 min, the surface morphology continued to change, producing a pattern of regular roughness (Fig. 7(C)). Morphological change continued with large cracks beginning to form in the surface (Fig. 7(D)) which grew until topographical stasis was reached (Fig. 7(E)) after over 2 h at <1% RH. The morphology of this surface was completely different to the initial smooth surface, consisting of a series of cracks with a rough surface in between. This is exemplified by the cross-section shown in Fig. 7(E), which shows a crack approximately 50 nm in depth.

Upon increasing the relative humidity to 50%, immediate changes were seen in surface morphology. Fig. 7(F) was recorded by a downward scan, beginning immediately after humidification began and being completed approximately 8 min later, by which time humidity had stabilised at 50 ± 3% RH. The morphology of the upper part if this image, recorded very soon after humidification commenced, is very similar to that seen at topographical stasis at <1% RH (see Fig. 7(E)), whereas the

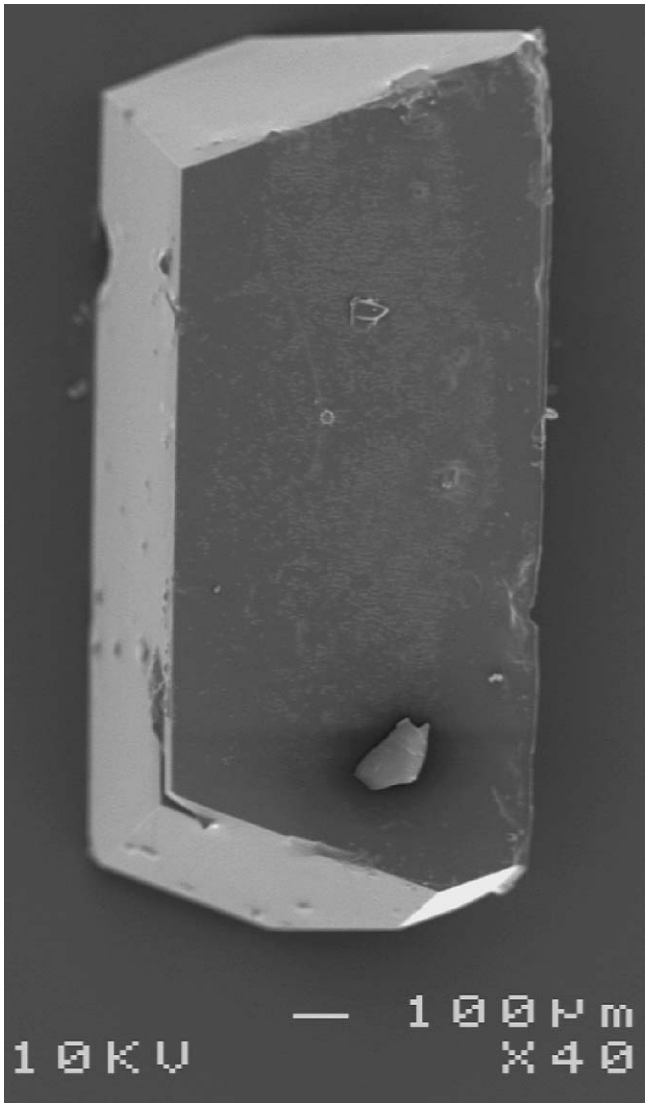

Fig. 5. Representative SEM image of recrystallised trehalose crystal.

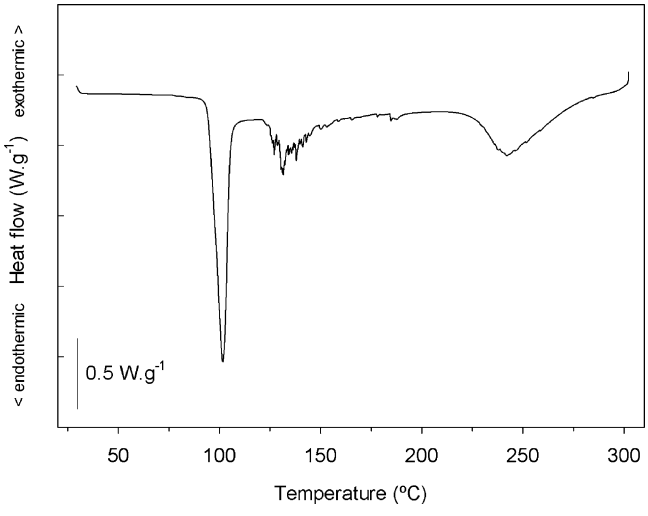

Fig. 6. Single crystal DSC thermogram obtained from recrystallised trehalose.

lower parts of the image, recorded a few minutes after humidity had been introduced, become progressively smoother. The bottom of the image is very similar in appearance to the image showing topographical stasis at 50% RH (Fig. 7(G)), although it should be noted that this surface is not as smooth as it was initially (Fig. 7(A)), as it still contains a number of cracks. This is exemplified by the large crack still present in the cross-section, the depth of which has decreased from approximately 50 nm to approximately 27 nm.

In order to glean quantitative information on the effect of humidity changes on the surface morphology of trehalose dihydrate crystals, the rugosity of each sequential AFM image was calculated and plotted against the time recorded upon completion of each scan (Fig. 8). This quantitative analysis confirmed the qualitative description of the images given above. After a period of stability, rugosity began a rapid increase approximately 45 min after relative humidity was decreased to <1%. It then stabilised at roughly nine times its initial value after approximately 2 h. When the relative humidity was increased to 50%, rugosity showed a rapid decrease (over less than 30 min) before stabilising at roughly three times its initial value.

SEM images of the surface of the recrystallised trehalose crystals showed a largely flat and smooth topography with a few minor imperfections (Fig. 9(A)). After reaching topographical stasis at <1% RH however, SEM images showed that cracks and pores had formed in the surface (Fig. 9(B)). These were comparable in size and shape to those observed by EC-AFM (Fig. 7(E)). The surface of the crystal that had reached topographical stasis at 50% RH proved difficult to image by SEM, as rounded features would rapidly appear during focusing and image capture (Fig. 9(C)). Despite these features, Fig. 9(C) clearly shows a series of cracks in the surface that appear to have partially closed when compared to those seen before exposure to 50% RH (Fig. 9(B)). This observation is consistent with the images obtained using EC-AFM (compare Fig. 7(E) and (G)).

3.8. Dynamic vapour sorption

The DVS profile of the recrystallised trehalose during exposure to a relative humidity cycle designed to mimic that used during EC-AFM is shown in Fig. 10. The trehalose mass was stable during the 15 min equilibration period at 35% RH, but showed a small, rapid decrease as soon as relative humidity was decreased to 0%. This is presumed to be due to the desorption of water molecules from the crystal surface. The mass then stabilised once again until approximately 50 min after the decrease to 0% RH, when it began a steady decrease, which was only reversed (from a minimum of 99.9776% of the original mass) when the humidity was increased to 50% RH. At this point the mass rapidly increased, reaching 99.9989% of the original mass after 30 min and an equilibrium mass of 99.9995% after an hour.

After exposure to this DVS cycle, the previously clear trehalose crystals were opaque with a “frosted” appearance (crystals removed from the EC-AFM after the same humidity cycle had a similar appearance). This effect can be seen in Fig. 11, which clearly shows that the crystal exposed to a humidity cycle transmitted much less light than an untreated crystal.

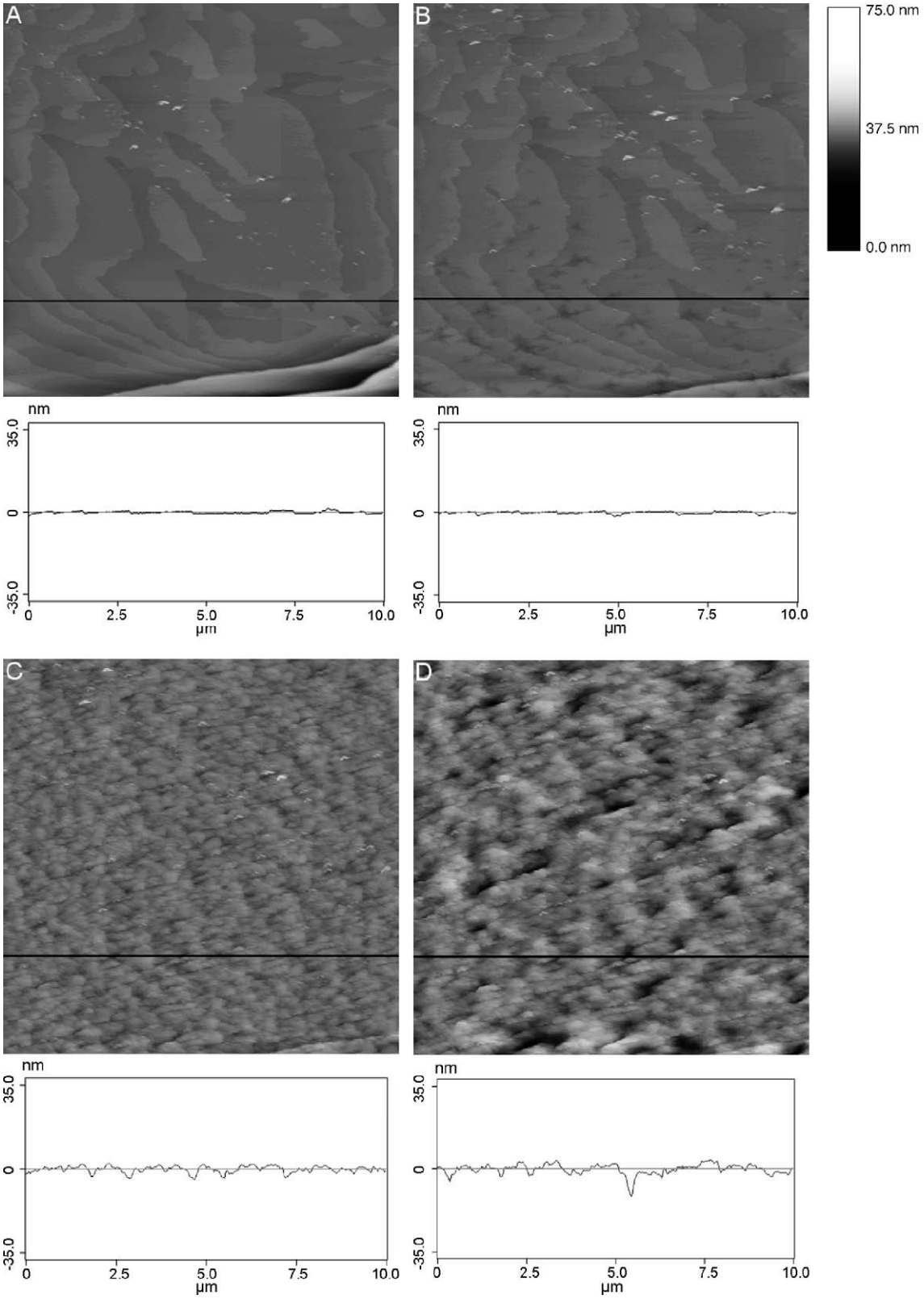

Fig. 7. Representative AFM Tapping Mode® images and cross-sections of a 10 μm × 10 μm portion of the surface of a recrystallised trehalose dihydrate crystal. (A) Under ambient conditions; (B) image completed 36 min after humidity reduced to <1% RH; (C) image completed 53 min after humidity reduced to <1% RH; (D) image completed 87 min after humidity reduced to <1% RH; (E) image completed 139 min after humidity reduced to <1% RH showing topographical stasis; (F) image completed 8 min after humidity increased to 50% RH showing transition from rough surface at the top of the image (captured first as scan direction was downwards) to a smoother surface at the bottom the image; (G) image completed 25 min after humidity increased to 50% RH showing topographical stasis. The bar shows the grayscale used to depict height in the images and the horizontal black line shows position of the cross-section, which is taken from the same position in each image.

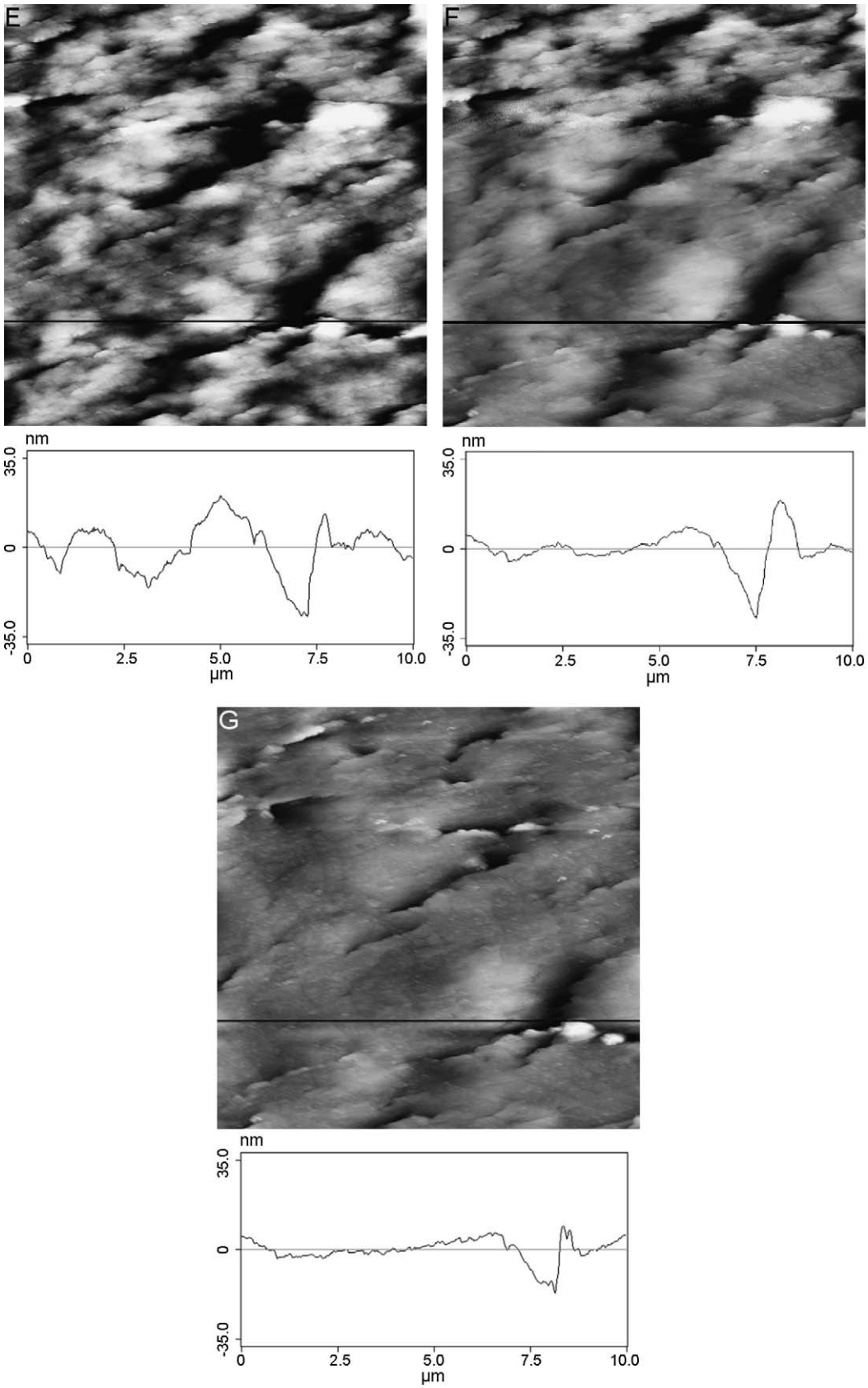

Fig. 7. (*Continued*).

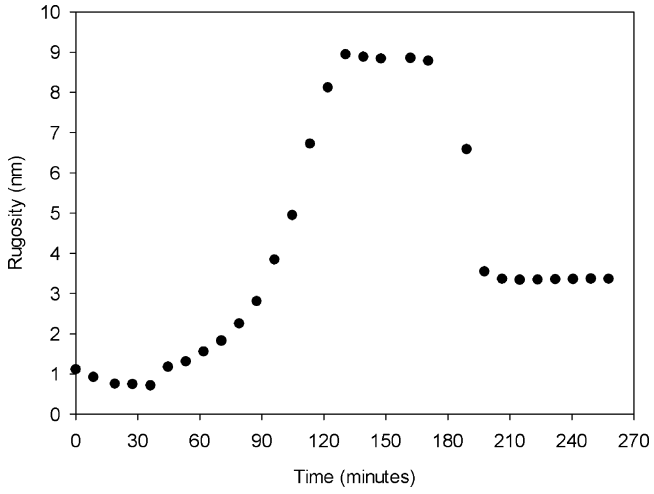

Fig. 8. Effect of relative humidity on the surface roughness of a trehalose dihydrate crystal, as measured by Tapping Mode® AFM. Relative humidity was reduced to <1% at 0 min and increased to 50 ± 3% at 180 min.

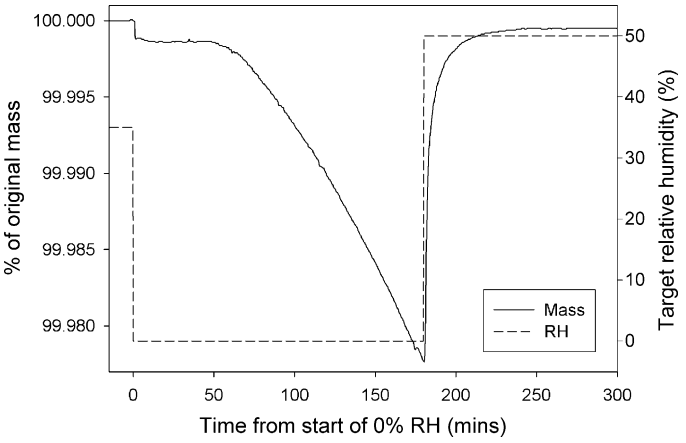

Fig. 10. DVS profile of recrystallised trehalose exposed to relative humidity cycle mimicking that used during EC-AFM.

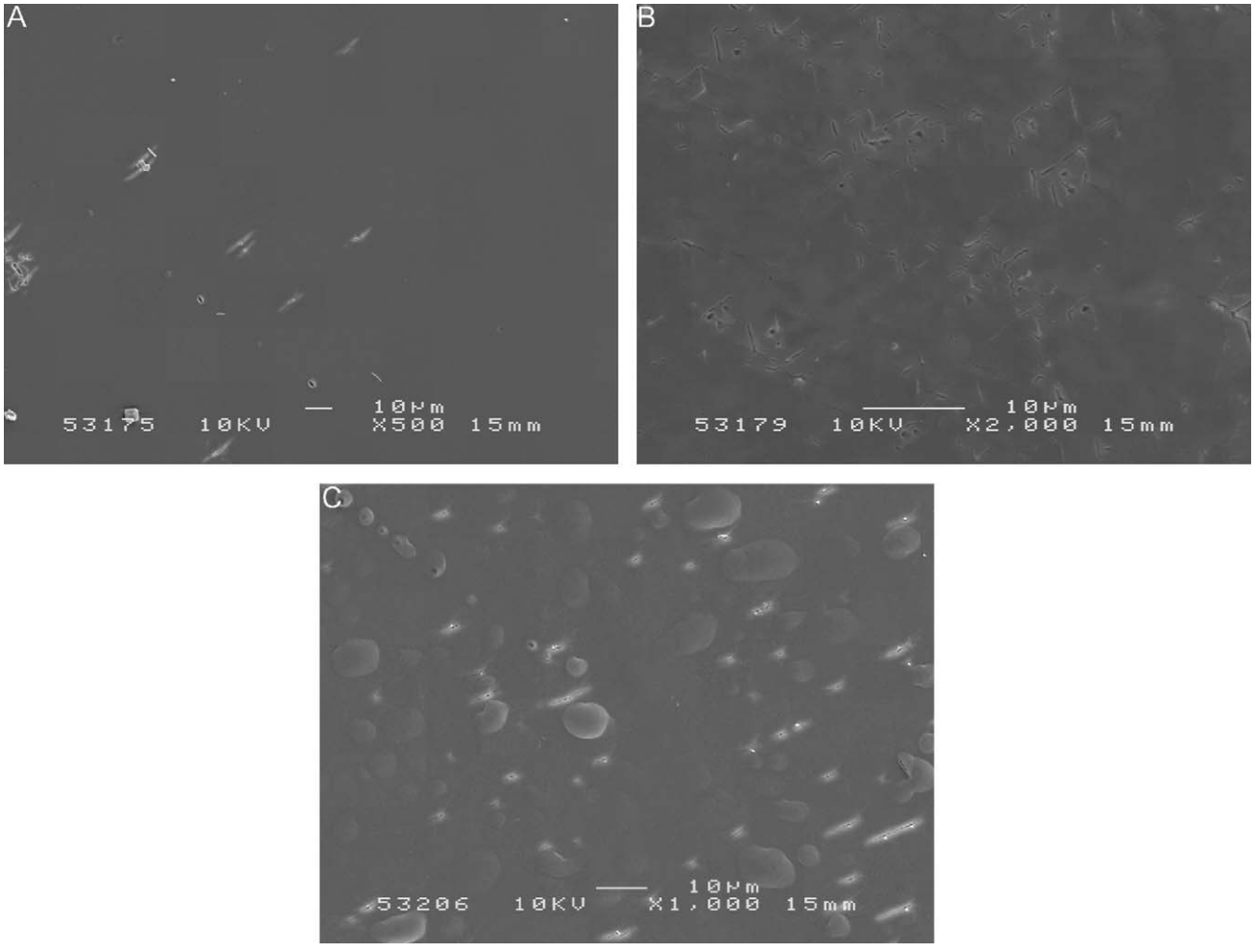

Fig. 9. Representative SEM images of the surface of recrystallised trehalose crystals. (A) Starting material; (B) after reaching topographical stasis at <1% RH in the EC-AFM; (C) after reaching topographical stasis at 50% RH in the EC-AFM. The rounded features in this image are artefacts caused by the imaging process.

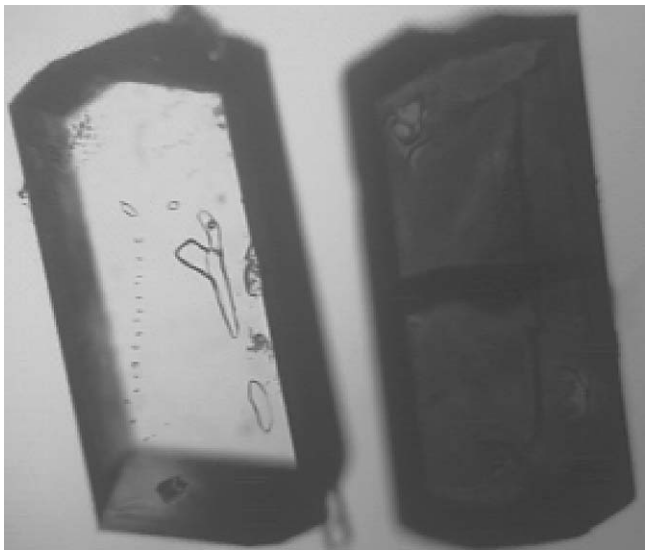

Fig. 11. Transmission light micrograph of recrystallised trehalose before (left-hand crystal) and after (right-hand crystal) exposure to DVS cycle described in text.

4. Discussion

The present work clearly demonstrates that trehalose dihydrate may be isothermally dehydrated to the α-form at ambient temperature under low humidity conditions. To the authors' knowledge, this is the first report of such a phenomenon, although it has previously been predicted that "dehydration could occur even below 40 °C, if dry conditions were satisfied" (Nagase et al., 2003). It is not unsurprising, however, that the α-form is produced by this dehydration, as this polymorph has previously been shown to be the product of a slow rate of water loss, as observed in this work (Willart et al., 2003).

It is clear from the small dehydration endotherm seen in the α-form thermogram and from the small peaks at 8.8° and 23.9° in the α-form XRPD spectrum that these samples also contained a small amount of trehalose dihydrate. It is hypothesised that this originated from two sources, incomplete initial dehydration (9.43% (w/w) mass loss was seen upon exposure to low humidity compared to 9.52% (w/w) water of crystallisation in trehalose dihydrate) and/or subsequent rehydration during the transfer from low humidity conditions to the DSC or XRPD instrument. It has previously been shown that >80% of the α-form will rehydrate to the dihydrate within 30 min of exposure to 43% RH and 25 °C (Nagase et al., 2002). It is therefore unsurprising that DSC and XRPD data should show evidence of rehydration having occurred during the 5–10 min it took to remove the dehydrated sample from low humidity conditions and prepare it for subsequent analysis under ambient laboratory conditions of approximately 31% RH and 24 °C. In addition, it was not possible to carry out XRPD under low humidity conditions, so rehydration would have continued during the analysis, which took approximately 30 min to sweep from 5° to 30°. This may explain why the dihydrate peak at 23.9° is more pronounced than that at 8.8° in the dehydrated trehalose spectrum.

The relative easy with which trehalose dihydrate can be dehydrated and subsequently rehydrated has been explained by reference to its crystal structure, in which "water molecules occupy adjacent positions along channels which lead to the crystal surface" (Sussich et al., 2001). Computer simulations suggest that water molecules are liberated from the crystal lattice by "hopping from site to site along these channels", at such a rate that the trehalose structure cannot relax into a more compact form (Sussich et al., 2001). In this way, the sugar architecture of trehalose dihydrate is thought to be maintained in the α anhydrous polymorph, as the "extensive interconnections between sugar molecules in the lattice can energetically support the lattice structure even after the water removal" (Sussich et al., 2001).

The observation by SEM of the formation of cracks in the surface of trehalose dihydrate upon dehydration is corroborated by the EC-AFM experiments. These revealed the propagation of cracks in real time, but also a nano-scale roughening of the surface too small to be observed by SEM. Both of these mechanisms contribute to the observed increase in surface roughness upon dehydration, a change which is not completely reversed by rehydration. It is postulated that these changes occur as water molecules liberated from the crystal structure within a trehalose particle force their way to the surface in order to escape into the surrounding low humidity environment. A similar observation has previously been made using hot-stage microscopy (Taylor and York, 1998a).

Comparison of the effect of 0% RH followed by 50% RH on recrystallised trehalose surface roughness (Fig. 8) and mass (Fig. 10) is striking. Rugosity was seen to increase approximately 45 min after relative humidity was decreased to 0%, whilst the decrease in mass was observed to begin after approximately 50 min. This confirms that the changes in surface morphology observed during EC-AFM are indeed caused by dehydration and suggests that there is a lag time before the dehydration of the large, recrystallised trehalose crystals begins. This was not observed with the trehalose powder used in the rest of this study, which may be due to its much larger surface area:volume ratio.

Rugosity stabilised approximately 2 h after relative humidity was decreased to 0%, whereas mass continued to decrease (showing no sign of reaching equilibrium) until the increase to 50% RH, at which point the maximum mass loss was only 0.0224%, as opposed to the 9.52% loss seen on completed dehydration. This suggests that changes in surface morphology are caused by the dehydration of only the surface layers of the crystal, so a sample of trehalose dihydrate may not have to be exposed to dehydrating conditions for very long to bring about this effect. Upon exposure to 50% RH, rugosity decreased to a stable level within 30 min, at which point mass had virtually returned to the original level (99.9989%). Equilibrium mass (99.9995%) was reached approximately an hour after relative humidity was increased to 50% and no further change in rugosity was observed during this time. This confirms that the change in surface morphology observed when relative humidity was increased to 50% was caused by rehydration of the dehydrated surface layers of the crystal. As rehydration was observed to be complete after an hour (by mass), at which point rugosity had stabilised at a

value roughly three times its initial value, it is also confirmed that the observed changes in surface morphology are irreversible by rehydration. This irreversibility is further established by the change in the visual appearance of recrystallised trehalose after dehydration and rehydration (Fig. 11), which is presumed to be caused by its rougher surfaces transmitting less light.

Given these findings, when considering the use of trehalose dihydrate in pharmaceutical formulations, there must be an appreciation that dehydration can occur at ambient temperatures and that this process causes rapid, irreversible changes in particle surface morphology before dehydration is complete, as such an event might cause serious changes in the behaviour and performance of the product. For example, the roughness of carrier particles in dry powder inhalation systems is widely acknowledged to affect formulation performance (Ganderton and Kassem, 1992; Prime et al., 1997). In addition, such formulations are commonly stored at low humidity, to prevent the formation of capillary bridges between particles. Were trehalose dihydrate used as the carrier in such a formulation, as it has been (under ambient conditions) in some investigations (Cline and Dalby, 2002; Hooton et al., in press), great care would be needed to avoid dehydration and the subsequent changes in rugosity and surface chemistry that might have a detrimental effect on formulation performance. Since rehydration occurs rapidly under ambient conditions (Nagase et al., 2002) without fully reversing morphological changes, it would not be sufficient to simply assay the final product to ensure it contained only the dihydrate, as this may mask a previous dehydration and change in surface roughness. Rather, the processing and storage conditions of trehalose dihydrate throughout its lifetime would need to be carefully controlled to prevent dehydration, otherwise severe batch-to-batch variation might be expected.

It should also be noted that various methods used for the basic characterisation of pharmaceutical powders, for example dynamic vapour sorption, surface area determination by nitrogen adsorption and helium pycnometry to determine true density, require samples to be dried prior to analysis. Under these conditions, it is likely that trehalose dihydrate will dehydrate, causing changes in sample mass, morphology and polymorph that might lead to erroneous results. The interpretation of such measurements should therefore be undertaken very carefully.

5. Conclusions

This study has demonstrated that trehalose dihydrate dehydrates to the α anhydrous polymorph when stored at low humidity and ambient temperature. This dehydration is accompanied by rapid changes in the morphology of particle surfaces (in particular the formation of cracks), which occur before dehydration is complete and are not fully reversible upon rehydration. This finding has particular relevance for the use of trehalose dihydrate as a pharmaceutical excipient in situations where surface properties are key to behaviour (for example, carrier-based dry powder inhalation formulations), as exposure of this material to conditions that may be obtained during processing or storage may lead to morphological changes and subsequent variations in formulation performance.

Acknowledgements

The authors wish to thank Barry Chapman of the Department of Physics, University of Bath, for his invaluable assistance in obtaining the XRPD spectra reported here. The authors gratefully acknowledge the Engineering Physical Sciences Research Council (EPSRC) and GlaxoSmithKline for the provision of a CASE award for MDJ and the EPSRC for funding the work of JCH and the purchase of the SEM.

References

Brown, G.M., Rohrer, D.C., Berking, B., Beevers, C.A., Gould, R.O., Simpson, R., 1972. The crystal structure of α,α-trehalose dihydrate from three independent X-ray determinations. Acta Crystallogr. Sect. B: Struct. Commun. 28, 3145–3158.

Cline, D., Dalby, R., 2002. Predicting the quality of powders for inhalation from surface energy and area. Pharm. Res. 19, 1274–1277.

Furuki, T., Kishi, A., Sakurai, M., 2005. De- and re-hydration behaviour of α,α-trehalose dihydrate under humidity-controlled atmospheres. Carbohydr. Res. 340, 429–438.

Ganderton, D., Kassem, N.M., 1992. Dry powder inhalers. In: Ganderton, D., Jones, T. (Eds.), Advances in Pharmaceutical Sciences, vol. 6. Academic Press, London, pp. 165–191.

Hooton, J.C., Jones, M.D., Price, R., in press. The use of a cohesive–adhesive force balance approach for predicting behaviour of novel sugar carriers for dry powder inhalation formulations. J. Pharm. Sci.

Jeffrey, G.A., Nanni, R., 1985. The crystal-structure of anhydrous α,α-trehalose at −150 degrees. Carbohydr. Res. 137, 21–30.

McGarvey, O.S., Craig, D.Q.M., Kett, V.L., 2003. Trehalose. In: Rowe, R.C., Sheskey, P.J., Weller, P.J. (Eds.), Handbook of Pharmaceutical Excipients. Pharmaceutical Press, London, pp. 657–658.

Nagase, H., Endo, T., Ueda, H., Nagai, T., 2003. Influence of dry conditions on dehydration of α,α-trehalose dihydrate. STP Pharma Sci. 13, 269–275.

Nagase, H., Endo, T., Ueda, H., Nakagaki, M., 2002. An anhydrous polymorphic form of trehalose. Carbohydr. Res. 337, 167–173.

Naini, V., Byron, P.R., Phillips, E.M., 1998. Physicochemical stability of crystalline sugars and their spray-dried forms: dependence upon relative humidity and suitability for use in powder inhalers. Drug Dev. Ind. Pharm. 24, 895–909.

Price, R., Young, P.M., 2004. Visualization of the crystallization of lactose from the amorphous state. J. Pharm. Sci. 93, 155–164.

Price, R., Young, P.M., Edge, S., Staniforth, J.N., 2002. The influence of relative humidity on particulate interactions in carrier-based dry powder inhaler formulations. Int. J. Pharm. 246, 47–59.

Prime, D., Atkins, P.J., Slater, A., Sumby, B., 1997. Review of dry powder inhalers. Adv. Drug Deliv. Rev. 26, 51–58.

Reisener, H.J., Goldschmid, H.R., Ledingham, G.A., Perlin, A.S., 1962. Formation of trehalose and polyols by wheat stem rust (*puccinia graminis tritici*) uredospores. Can. J. Biochem. Physiol. 40, 1248–1251.

Sussich, F., Bortoluzzi, S., Cesaro, A., 2002. Trehalose dehydration under confined conditions. Thermochim. Acta 391, 137–150.

Sussich, F., Princivalle, F., Cesaro, A., 1999. The interplay of the rate of water removal in the dehydration of α,α-trehalose. Carbohydr. Res. 322, 113–119.

Sussich, F., Skopec, C., Brady, J., Cesaro, A., 2001. Reversible dehydration of trehalose and anhydrobiosis: from solution state to an exotic crystal? Carbohydr. Res. 334, 165–176.

Sussich, F., Urbani, R., Princivalle, F., Cesaro, A., 1998. Polymorphic amorphous and crystalline forms of trehalose. J. Am. Chem. Soc. 120, 7893–7899.

Taga, T., Senma, M., Osaki, K., 1972. The crystal and molecular structure of trehalose dihydrate. Acta Crystallogr. Sect. B: Struct. Commun. B28, 3258–3263.

Taylor, L.S., Williams, A.C., York, P., 1998. Particle size dependent molecular rearrangements during the dehydration of trehalose dihydrate—in situ ft-raman spectroscopy. Pharm. Res. 15, 1207–1214.

Taylor, L.S., York, P., 1998a. Characterization of the phase transitions of trehalose dihydrate on heating and subsequent dehydration. J. Pharm. Sci. 87, 347–355.

Taylor, L.S., York, P., 1998b. Effect of particle size and temperature on the dehydration kinetics of trehalose dihydrate. Int. J. Pharm. 167, 215–221.

Willart, J.F., Danede, F., De Gusseme, A., Descamps, M., Neves, C., 2003. Origin of the dual structural transformation of trehalose dihydrate upon dehydration. J. Phys. Chem. B 107, 11158–11162.

Willart, J.F., De Gusseme, A., Hemon, S., Descamps, M., Leveiller, F., Rameau, A., 2002. Vitrification and polymorphism of trehalose induced by dehydration of trehalose dihydrate. J. Phys. Chem. B 106, 3365–3370.